

DYNAMIC TRANSITIONS OF THE SWIFT-HOHENBERG EQUATION WITH THIRD-ORDER DISPERSION

KEVIN LI

ABSTRACT. The Swift-Hohenberg equation is ubiquitous in the study of bistable dynamics. In this paper, we study the dynamic transitions of the Swift-Hohenberg equation with a third-order dispersion term in one spacial dimension with a periodic boundary condition. As a control parameter crosses a critical value, the trivial stable equilibrium solution will lose its stability, and undergoes a dynamic transition to a new physical state, described by a local attractor. The main result of this paper is to fully characterize the type and detailed structure of the transition using dynamic transition theory [7]. In particular, employing techniques from center manifold theory, we reduce this infinite dimensional problem to a finite one since the space on which the exchange of stability occurs is finite dimensional. The problem then reduces to analysis of single or double Hopf bifurcations, and we completely classify the possible phase changes depending on the dispersion for every spacial period.

CONTENTS

1. Introduction	1
2. Preliminaries	3
3. Dynamic Transitions	10
4. Real Center Manifold Function and Numerical Results	16
Acknowledgements	23
References	24

1. INTRODUCTION

The standard Swift-Hohenberg equation was introduced to describe the onset of Rayleigh-Benard convection, which considers a horizontal layer of viscous fluid heated from below. It is given by

$$\frac{\partial u}{\partial t} = -(1 + \Delta)^2 u + \lambda u - u^3,$$

and is crucial to the study of non-equilibrium physic due to the natural formation of convection patterns as the fluid is heated. As the control parameter λ increases, the equation exhibits distinct pattern forming behavior [1, 3]. Spacial and temporal patterns occur when systems transition from a basic stable state and bifurcates to

Date: March 17, 2024.

nontrivial attractors when the control parameter crosses a critical value. The phase transition dynamics of the standard Swift-Hohenberg equation is well understood in one and two spacial dimensions [1]. Beyond hydrodynamics, this fourth-order equation has a plethora of applications in bistable dynamics. Of particular interest to us is when a ring cavity made of optical fibers is driven by a beam. When the beam is operating near the resonant frequency of the cavity, the dynamics exhibited by the the cavity is modelled by the Swift-Hohenberg equation with a third-order dispersion term [2].

In this paper, we fully characterize the phase transition dynamics of the Swift-Hohenberg equation with a third-order dispersion in one spacial dimension, given by

$$(1) \quad \begin{cases} u_t = \lambda u - (1 + \partial_x^2)^2 u + \sigma \partial_x^3 u + bu^2 - u^3 & \text{for } x \in [0, \ell], t \geq 0 \\ u(t, 0) = u(t, \ell) & \forall t \geq 0. \end{cases}$$

Let \mathbb{T} denote the torus of measure ℓ . Then we can consider

$$L_\lambda = \lambda - (1 + \partial_x^2)^2 + \sigma \partial_x^3$$

as an operator from $H^4(\mathbb{T}) \rightarrow L^2(\mathbb{T})$. Note that the nonlinear mapping $G(u, \lambda) = bu^2 - u^3$ can be expanded as $G(u, \lambda) = G_2(u, \lambda) + o(\|u\|_{H^4(\mathbb{T})}^2)$ where $G_2(u_1, u_2, \lambda) = bu_1 u_2$ is a one parameter family of bilinear mappings. Since we have the embedding $H^4(\mathbb{T}) \hookrightarrow C^3(\mathbb{T})$, then Eq. (1) with the boundary condition can be recasted as

$$(2) \quad u_t = L_\lambda u + G(u, \lambda).$$

Small perturbation of the control parameter, λ , about a critical value leads to significantly different dynamics near the trivial equilibrium point.

To analyze the exchange of stability that occurs across a critical value of λ , we use the framework of dynamic transition theory set forth by Ma and Wang [7]. In equilibrium thermodynamics, the standard characterization of phase transition is through the Ehrenfest classification, where transitions are classified based on the regularity across a critical value in the control parameter with respect to some thermodynamic potential. For example, as the temperature crosses the 0°C threshold for a sample of water, the first order derivative of the Gibbs potential function is discontinuous at $T = 0^\circ\text{C}$, so it is a first order transition. This largely hides the dynamic properties of the system in state space. For general dynamical systems, it is natural to analyze how an attractor loses stability as the control parameter crosses a critical value, in relations to local attractors.

The paper will be organized as follows. We start with some preliminaries, in which we give an overview of general dynamic transition theory, as well as a general description of the dynamic transitions that accompany a Hopf and double Hopf bifurcation. After the preliminaries, the main theorem will be given by Theorem 2.4, which will fully characterize the dynamic transitions of the Swift-Hohenberg equation with third-order dispersion in one dimension. In particular, we will show in Section 3 that for $\ell \leq 2\pi/\sqrt{2}$, the transition and dynamics are completely determined by whether b is non-zero in Eq. (1). For $\ell \leq 2\pi/\sqrt{2}$, we will either end up

with a simple Hopf bifurcation or a double Hopf bifurcation, the behaviors of which will be fully characterized in Theorem 2.2 and Theorem 2.3.

2. PRELIMINARIES

We start with a general dynamical system. Let X_1 and X be two Banach spaces such that $X_1 \subset X$ is a compact inclusion. Consider the nonlinear evolution equation

$$(3) \quad \frac{\partial u}{\partial t} = L_\lambda u + G(u, \lambda), \quad u(0) = u_0$$

and L_λ is a one parameter family of linear completely continuous fields depending continuously on λ , i.e.

$$(4) \quad \begin{array}{ll} L_\lambda = -A + B_\lambda & \text{is a sectorial operator} \\ A : X_1 \rightarrow X & \text{is a linear homeomorphism} \\ B_\lambda : X_1 \rightarrow X & \text{linear compact operators parameterized by } \lambda. \end{array}$$

In this case, we can define fractional power operators L_λ^α with domain $X_\alpha = D(L_\lambda^\alpha)$. We further assume that $G(\cdot, \lambda) : X_\alpha \rightarrow X$ is a C^r bounded mapping for some $0 \leq \alpha < 1$ and $r \geq 1$, and depends continuously on λ , and for all $\lambda \in \mathbb{R}$,

$$(5) \quad G(u, \lambda) = o(\|u\|_{X_\alpha})$$

This implies that $u = 0$ is a trivial equilibrium point. Clearly there is no loss of generality in this assumption since we may just shift the system by a constant.

Definition 1. [7] The system given by Eq. (3) satisfying Eq. (4) undergoes a dynamic transition at $\lambda = \lambda_0$ if the following conditions hold:

- (1) if $\lambda < \lambda_0$, Eq. (3) is locally asymptotically stable at $u = 0$,
- (2) if $\lambda > \lambda_0$, $\text{codim}(\Gamma_\lambda) \geq 1$ where Γ_λ is the stable manifold of Eq. (3) about $u = 0$ for λ , and there exists a neighborhood $U \subset X$ of $u = 0$ independent of λ such that for any $u_0 \in U \setminus \Gamma_\lambda$, the solution u_λ with initial value u_0 satisfies

$$\limsup_{t \rightarrow \infty} \|u_\lambda(t, u_0)\|_X \geq \delta(\lambda) > 0, \quad \lim_{\lambda \rightarrow \lambda_0^+} \delta(\lambda) \geq 0.$$

This amounts to saying that a dynamic transition happens when the equilibrium point at $u = 0$ loses stability across λ_0 . The simplest way this occurs is if eigenvalues of L_λ crosses the imaginary axis as λ crosses λ_0 . If such an exchange of stability occurs, then we can classify the dynamic transition into three categories.

Theorem 2.1. [7] Let the eigenvalues of L_λ be given by $\{\beta_i(\lambda) : i = 1, 2, \dots\}$, and suppose

$$(6) \quad \begin{array}{ll} \text{Re}(\beta_i) \begin{cases} < 0 & \text{if } \lambda < \lambda_0 \\ = 0 & \text{if } \lambda = \lambda_0 \\ > 0 & \text{if } \lambda > \lambda_0 \end{cases} & 1 \leq i \leq m \\ \text{Re}(\beta_i) < 0 & i > m, \end{array}$$

then Eq. (3) undergoes a dynamic transition at $\lambda = \lambda_0$, and is one of the following three types:

- (i) there exists a neighborhood $U \subset X$ of $u = 0$ and dense subsets \tilde{U}_λ so that for any $u_0 \in \tilde{U}_\lambda$, solution $u_\lambda(t, u_\lambda)$ satisfies

$$\lim_{\lambda \rightarrow \lambda_0^+} \limsup_{t \rightarrow \infty} \|u_\lambda(t, u_0)\| = 0$$

- (ii) there exists a neighborhood $U \subset X$ of $u = 0$ and dense subset \tilde{U}_λ and an $\epsilon > 0$ so that for any $\lambda_0 < \lambda < \lambda_0 + \epsilon$ and any $u_0 \in \tilde{U}_\lambda$, solution $u_\lambda(t, u_\lambda)$ satisfies

$$\limsup_{t \rightarrow \infty} \|u_\lambda(t, u_0)\| \geq \delta > 0$$

for some fixed δ independent of λ .

- (iii) there exists a neighborhood $U \subset X$ of $u = 0$ such that for any $\lambda_0 < \lambda < \lambda_0 + \epsilon$ for some $\epsilon > 0$, we have a decomposition U_λ^1 and U_λ^2 so that $\bar{U} = \bar{U}_\lambda^1 \cup \bar{U}_\lambda^2$ and $U_\lambda^1 \cap U_\lambda^2 = \emptyset$, and

$$\begin{aligned} \lim_{\lambda \rightarrow \lambda_0^+} \limsup_{t \rightarrow \infty} \|u_\lambda(t, u_0)\| &= 0 & u_0 \in U_\lambda^1 \\ \limsup_{t \rightarrow \infty} \|u_\lambda(t, u_0)\| &\geq \delta > 0 & u_0 \in U_\lambda^2 \end{aligned}$$

for some fixed δ independent of λ .

These transitions are called *continuous*, *catastrophic*, and *mixed* transitions respectively, and we call β_i with $1 \leq i \leq m$ the critical eigenvalues. A proof of the theorem is given by Ma-Wang [7]. Physically, a phase transition occurs when a system leaves a basic local attractor to another, called the transition states, as a system parameter λ crosses the threshold value λ_0 . In a continuous transition, the transition states attracts a neighborhood of the basic state. In a catastrophic transition, the transition states are local attractors away from the basic state. Note that this classification has a natural relation to the Ehrenfest classification for equilibrium phase transitions. In particular, catastrophic implies first order since stability is lost abruptly and jumps away from the basic state. Continuous transition corresponds directly to second order transition. For the complete relation between the two classifications, see [7].

If the system satisfies the conditions given in (6), it suffices to analyze the dynamics on the finite dimensional center manifold tangent to the subspace spanned by eigenvectors β_i with $1 \leq i \leq m$, since the space orthogonal to the center subspace is stable. Hence any solution with initial value near 0 will be attracted towards the center manifold. Furthermore, the center manifold is tangent to the center subspace, so the dynamics on the center manifold near the trivial equilibrium point is equivalent to the dynamics of the solution projected onto the center subspace. In particular, we have the following two useful theorems that extend the Hopf bifurcation theorem.

Theorem 2.2. [4, 5, 7, 8] *Consider a system in the form of Eq. (3) that satisfies (4). Assume that there are two critical eigenvalues that are complex simple, β_1 and $\bar{\beta}_1$, so that assumption (6) holds. Further assume that the solutions to the system projected onto the critical eigenvector ϕ_1 for sufficiently small initial value and λ*

near λ_0 satisfies

$$(7) \quad \frac{dz}{dt} = \beta_1(\lambda)z + P(\lambda)z|z|^2 + o(|z|^3)$$

where z is the amplitude of projection of the solution and $P(\lambda)$ is continuously differentiable near $\lambda = \lambda_0$. $P = P(\lambda_0) \in \mathbb{C}$ is a constant called the transition number. Then the transition of the system is completely characterized by the dynamics at $\lambda = \lambda_0$. In particular, we have the following characterization:

- (i) If $\text{Re}(P) < 0$, the system undergoes a continuous transition to a local attractor σ_λ homological to S^1 , and the basic steady state solution $u = 0$ bifurcates to a stable periodic solution u_λ on $\lambda > \lambda_0$.
- (ii) If $\text{Re}(P) > 0$, the system undergoes a catastrophic transition, and the basic steady state solution $u = 0$ bifurcates to an unstable periodic solution u_λ on $\lambda < \lambda_0$.
- (iii) u_λ in both (1) and (2) have the approximation

$$(8) \quad u_\lambda(x, t) = 2 \left(\frac{-\text{Re } \beta_1(\lambda)}{\text{Re } P} \right)^{1/2} \text{Re}(e^{i\omega t} \phi_1) + o(\text{Re } \beta)^{1/2}$$

where

$$\omega = \text{Im } \beta_1 - \text{Im } P \frac{\text{Re } \beta_1}{\text{Re } P}$$

Proof. Making the substitution $z = \rho(t)e^{i\gamma(t)}$ where ρ and γ are real-valued functions and $\rho(t) > 0$, we find that the real part of the differential equation is given by

$$(9) \quad \rho'(t) = \text{Re } \beta_1(\lambda)\rho(t) + \text{Re } P(\lambda)\rho(t)^3 + o(|z|^3).$$

At $\lambda = \lambda_0$, $\text{Re } \beta_1(\lambda_0) = 0$, so clearly $\rho = 0$ is an asymptotically stable equilibrium point if $\text{Re } P < 0$, and an unstable equilibrium point if $\text{Re } P > 0$. Thus the transition is continuous if $\text{Re } P < 0$ and catastrophic if $\text{Re } P > 0$. By the Hopf bifurcation theorem, the stable equilibrium must bifurcate to a periodic orbit for $\lambda > \lambda_0$ if $\text{Re } P > 0$. From Eq. (9), we see that $z = \frac{-\text{Re } \beta_1(\lambda)}{\text{Re } P} e^{i\gamma(t)} + o(\text{Re } \beta)^{1/2}$. Taking the imaginary part in the substitution, we find

$$\gamma'(t) = \text{Im } \beta + \text{Im } P \rho^2(t),$$

from which it follows that $\gamma(t) = \omega t$. □

Theorem 2.3. Consider a system in the form of Eq. (3) that satisfies (4). Assume that there are 2 pairs of conjugate critical eigenvalues, $\beta_1, \beta_2, \bar{\beta}_1$, and $\bar{\beta}_2$, and that assumption (6) holds. Further assume that the solution of the system projected onto the critical eigenvectors ϕ_1 and ϕ_2 for sufficiently small initial value and λ near λ_0 satisfies

$$(10) \quad \frac{dz_1}{dt} = \beta_1(\lambda)z_1 + z_1(A(\lambda)|z_1|^2 + B(\lambda)|z_2|^2) + o((|z_1| + |z_2|)^3)$$

$$(11) \quad \frac{dz_2}{dt} = \beta_2(\lambda)z_2 + z_2(C(\lambda)|z_1|^2 + D(\lambda)|z_2|^2) + o((|z_1| + |z_2|)^3)$$

where z_1 and z_2 are the amplitude of projection onto ϕ_1 and ϕ_2 respectively. A , B , C , and D are continuously differentiable near $\lambda = \lambda_0$, and evaluated at λ_0 , these are called the transition numbers, and we define $m_1 = -\operatorname{Re} A / \operatorname{Re} B$ and $m_2 = -\operatorname{Re} C / \operatorname{Re} D$. The transition is then completely characterized by the dynamics of the reduced system (10) - (11), and we have the following classification:

- (i) If $\operatorname{Re} A < 0$ and $\operatorname{Re} B < 0$, then
 - (a) if $\operatorname{Re} C < 0$ and $\operatorname{Re} D < 0$, then the transition is continuous,
 - (b) if $\operatorname{Re} C < 0$ and $\operatorname{Re} D > 0$, then the transition is mixed if $\operatorname{Re} A - \operatorname{Re} C > 0$ and catastrophic if $\operatorname{Re} A - \operatorname{Re} C \leq 0$,
 - (c) if $\operatorname{Re} C > 0$ and $\operatorname{Re} D < 0$, then the transition is continuous,
 - (d) if $\operatorname{Re} C > 0$ and $\operatorname{Re} D > 0$, then the transition is catastrophic.
- (ii) If $\operatorname{Re} A < 0$ and $\operatorname{Re} B > 0$, then
 - (a) if $\operatorname{Re} C < 0$ and $\operatorname{Re} D < 0$, then the transition is continuous,
 - (b) if $\operatorname{Re} C > 0$ and $\operatorname{Re} D < 0$, then the transition is continuous if $m_1 > m_2$ and catastrophic if $m_1 < m_2$.
 - (c) if $\operatorname{Re} C < 0$ and $\operatorname{Re} D > 0$, then the transition is continuous if $m_1 < m_2$. Furthermore if $m_2 > m_1$, then the transition is mixed if $\frac{\operatorname{Re} A - \operatorname{Re} C}{\operatorname{Re} D - \operatorname{Re} B} > 0$, and catastrophic if $\frac{\operatorname{Re} A - \operatorname{Re} C}{\operatorname{Re} D - \operatorname{Re} B} < 0$.
 - (d) if $\operatorname{Re} C > 0$ and $\operatorname{Re} D > 0$, then the transition is catastrophic.
- (iii) If $\operatorname{Re} A > 0$ and $\operatorname{Re} B < 0$, then
 - (a) if $\operatorname{Re} C < 0$ and $\operatorname{Re} D < 0$, the transition is mixed if $\operatorname{Re} D - \operatorname{Re} B > 0$ and catastrophic otherwise.
 - (b) if $\operatorname{Re} C < 0$ and $\operatorname{Re} D > 0$, then the transition is catastrophic if $m_1 > m_2$.
 - (c) if $\operatorname{Re} C > 0$ and $\operatorname{Re} D < 0$, then the transition is mixed if $\frac{\operatorname{Re} D - \operatorname{Re} B}{\operatorname{Re} A - \operatorname{Re} C} > 0$ and catastrophic otherwise.
 - (d) if $\operatorname{Re} C > 0$ and $\operatorname{Re} D > 0$, then the transition is catastrophic.
- (iv) if $\operatorname{Re} A > 0$ and $\operatorname{Re} B > 0$, then the transition is catastrophic.

Furthermore, if the transition is continuous, the trivial stable equilibrium point bifurcates to an S^3 attractor for $\lambda > \lambda_0$.

Proof. We employ the same change of variables as [4]. Let

$$z_1(t) = \sqrt{\rho_1(t)} e^{i\gamma_1(t)} \quad z_2(t) = \sqrt{\rho_2(t)} e^{i\gamma_2(t)}$$

where γ_i and ρ_i for $i = 1, 2$ are real functions, and $\rho_i(t) \geq 0$. Then substituting into Eq. (10) and Eq. (11) then taking the real part, we find that

$$\begin{aligned} \dot{\rho}_1 &= 2\rho_1(\operatorname{Re} \beta_1 + \operatorname{Re}(A)\rho_1 + \operatorname{Re}(B)\rho_2 + O(\rho_1^2 + \rho_2^2)), \\ \dot{\rho}_2 &= 2\rho_2(\operatorname{Re} \beta_1 + \operatorname{Re}(C)\rho_1 + \operatorname{Re}(D)\rho_2 + O(\rho_1^2 + \rho_2^2)). \end{aligned}$$

Note that since $\dot{\rho}_1|_{\rho_1=0} = 0$ and $\dot{\rho}_2|_{\rho_2=0} = 0$, any initial value of (ρ_1, ρ_2) will remain in the first quadrant. It is clear that if all trajectories with initial value in the first quadrant tend to ∞ as $t \rightarrow \infty$, then the transition will be catastrophic, and if all such trajectories tend to 0, then the transition will be continuous. Otherwise it is mixed.

- (i) First consider the case $\text{Re } A, \text{Re } B < 0$. Then $\dot{\rho}_1 < 0$ in the first quadrant. Thus if $\text{Re } C, \text{Re } D < 0$, we have a continuous transition, and if $\text{Re } C, \text{Re } D < 0$, we have a catastrophic transition.

Now suppose $\text{Re } C > 0$ and $\text{Re } D < 0$. Then on the left side of the line $\rho_2 = m_2\rho_1$, $\dot{\rho}_2 < 0$, and on the right side $\dot{\rho}_2 > 0$. Clearly every trajectory that starts on the left side tends to 0. Since $|\dot{\rho}_1|$ increases as ρ_2 increases, every trajectory that starts on the right side must enter the left side, and thus tends to 0 as $t \rightarrow \infty$.

Finally consider $\text{Re } C < 0$ and $\text{Re } D > 0$. In this case, on left side of the line $\rho_2 = m_2\rho_1$, we have $\dot{\rho}_2 > 0$ and on the right we have $\dot{\rho}_2 < 0$. Any solution starting on the left side of the line must then tend to ∞ . If $\text{Re } A - \text{Re } C > 0$, then the line $\rho_2 = k\rho_1$ where $k = \frac{\text{Re } A - \text{Re } C}{\text{Re } D - \text{Re } B}$ has positive slope and thus passes through the first quadrant. In particular, $k < m_2$, along this line, $\dot{\rho}_2/\dot{\rho}_1 = k$. Therefore any trajectory with initial value below this line must tend to 0, hence the transition is mixed. On the other hand, if $\text{Re } A - \text{Re } C \leq 0$, then $\dot{\rho}_2/\dot{\rho}_1 < \rho_2/\rho_1$ for every point below the line $\rho_2 = m_2\rho_1$. Therefore all such trajectory must enter the region above the line at some $t > 0$, thus the transition must be catastrophic.

- (ii) Now consider the case $\text{Re } A < 0$ and $\text{Re } B > 0$. Then on the left side of the line $\rho_2 = m_2\rho_1$, $\dot{\rho}_1 > 0$, and on the right side, $\dot{\rho}_2 < 0$. If $\text{Re } C < 0$ and $\text{Re } D < 0$, this is identical to case 1(c), so the transition is continuous.

If $\text{Re } C > 0$ and $\text{Re } D < 0$, then above the line $\rho_2 = m_2\rho_1$, $\dot{\rho}_2 < 0$, and below, we have $\dot{\rho}_2 > 0$. In Fig. 1, we clearly see that there are two cases depending on if $m_1 < m_2$ or $m_1 > m_2$. The first quadrant is divided into three regions by the two lines. Label the regions I, II, and III from left to right. In either case, initial values in regions I and III will end up in region II. In the case $m_1 < m_2$, initial values in region II will tend to ∞ , and in the case $m_1 > m_2$, initial values in region II will tend to 0. Therefore we have catastrophic transition in the former case and continuous in the latter.

A combination of the analysis of 2(b) and 1(b) proves 2(c). Finally if $\text{Re } C > 0$ and $\text{Re } D > 0$, the trajectory will necessarily tend to ∞ along the ρ_2 direction, hence it is catastrophic.

- (iii) and (iv) can be shown through identical analysis. See [5] for a proof of the S^3 structure of the bifurcated attractor. \square

For the sake of completeness completeness, Theorem 2.3 fully characterized every possible combination of the transition number. We will see in Section 3.4 that our Swift-Hohenberg system with dispersion will only require analysis of a subset of these combinations.

Now to characterize the transitions of Eq. (1), we must identify the eigenvalues that first cross the imaginary axis of the associated operator L_λ defined in Section 1. Expanding $L_\lambda u = \beta(\lambda)u$ as a Fourier series, we find that we have eigenvalues

$$\beta_n(\lambda) = \lambda - \left(1 - \frac{4\pi^2 n^2}{\ell^2}\right)^2 - i\sigma \frac{8\pi^3}{\ell^3} n^3$$

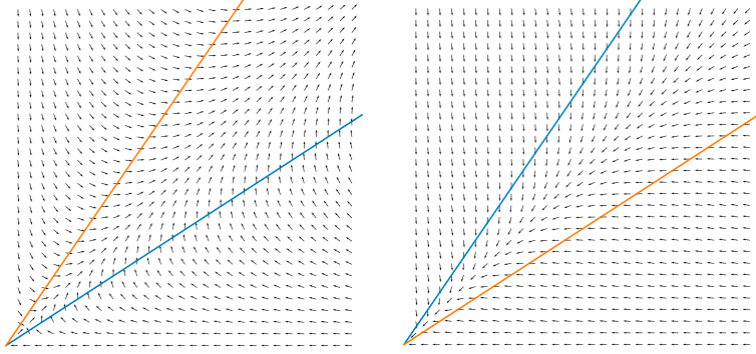


FIGURE 1. These vector fields show the general shape of the case $\operatorname{Re} C > 0$ and $\operatorname{Re} D < 0$. The blue line is the line $\rho_2 = m_1 \rho_1$ and the orange line is the line $\rho_2 = m_2 \rho_1$.

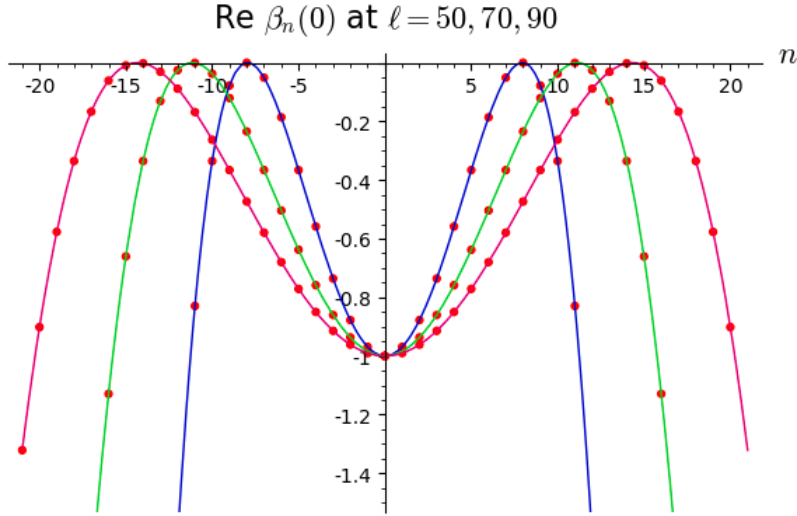


FIGURE 2. Plot of $\operatorname{Re} \beta_n(0)$ for various ℓ . One can see from the figure that for large ℓ , the maximas over $n \in \mathbb{Z}$ are attained at one or two pairs of conjugate eigenvalues. For sufficiently small ℓ , $\beta_0(0)$ will be the maximum eigenvalue.

with corresponding eigenvectors

$$\phi_n(x) = e^{2\pi i n x / \ell}.$$

for $n \in \mathbb{Z}$. It is clear that $\arg \max_{n \in \mathbb{Z}} \operatorname{Re} \beta_n(0)$ is always a finite set with some cardinality $m(\ell)$, and it consists of the first eigenvalues to cross the imaginary axis (see Fig. 2). Observe that $\beta_0(0) = -1$, and for all $\ell < 2\pi/\sqrt{2}$, $\operatorname{Re} \beta_n(0) < -1$ for all

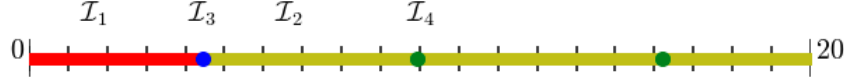


FIGURE 3. A visual of the partition. \mathcal{I}_1 , \mathcal{I}_2 , \mathcal{I}_3 , and \mathcal{I}_4 are encoded by the colors red, yellow, blue, and green respectively.

$n \neq 0$, and for $\ell > 2\pi/2$, $\operatorname{Re} \beta_1(0) > -1$. Therefore

$$\begin{cases} m(\ell) = 1 & \ell < 2\pi/\sqrt{2} \\ m(\ell) \geq 2 & \ell \geq 2\pi/\sqrt{2} \end{cases}.$$

In particular, $m(2\pi/\sqrt{2}) = 3$ since $\operatorname{Re} \beta_1 = \operatorname{Re} \beta_{-1} = \operatorname{Re} \beta_0 = -1$. When $\ell > 2\pi/\sqrt{2}$, note that $\operatorname{Re} \beta_1(0) > -1$, so for such ℓ , we either have one or two pairs of conjugate eigenvalues that first cross the imaginary axis as λ increases. We then define the following partition of \mathbb{R}^+ :

Definition 2. Let $\mathcal{I}_1 \cup \mathcal{I}_2 \cup \mathcal{I}_3 \cup \mathcal{I}_4 = \mathbb{R}^+$ so that for any $\ell \in \mathcal{I}_i$, $m(\ell) = i$. In particular, \mathcal{I}_1 is an open interval, \mathcal{I}_2 is a union of open intervals, \mathcal{I}_3 is a single point, and \mathcal{I}_4 is a discrete set (see Fig. 3).

For convenience, we define the inverted length

$$\rho := \frac{2\pi}{\ell}$$

If $\beta_k(0) \in \arg \max_{n \in \mathbb{Z}} \operatorname{Re} \beta_n(0)$, then at $\lambda_0 = (1 - (k\rho)^2)^2$, then we have a dynamic transition. Now we are ready to state the main theorem.

Theorem 2.4. *The Swift-Hohenberg equation with third-order dispersion always undergoes a dynamic transition across $\lambda = \lambda_0$, and the transitions can be characterized by the following:*

- (i) *if $\ell \in \mathcal{I}_1$, then the transition is mixed if $b \neq 0$, and is continuous if $b = 0$. In particular, if $b = 0$, the basic state at $u = 0$ will bifurcate to two stable equilibrium points for $\lambda > \lambda_0 = 1$.*
- (ii) *if $\ell \in \mathcal{I}_2$, then there exists k such that $\operatorname{Re} \beta_k(\lambda_0) = 0$ where $\lambda_0 = (1 - (k\rho)^2)^2$. The transition is continuous if*

$$\frac{2b^2(15(k\rho)^4 - 6(k\rho)^2)}{(15(k\rho)^4 - 6(k\rho)^2)^2 + (6\sigma(k\rho)^3)^2} + \frac{4b^2}{1 - \lambda_0} - 3 < 0,$$

and catastrophic if the inequality is reversed. If continuous, the basic attractor at $u = 0$ bifurcates to a stable periodic orbit for $\lambda > \lambda_0$, and if catastrophic, the basic attractor at $u = 0$ bifurcates to an unstable periodic orbit for $\lambda < \lambda_0$.

- (iii) *if $\ell \in \mathcal{I}_3$, then the transition is mixed if $b \neq 0$, and is continuous if $b = 0$. In particular, if $b = 0$, the basic state at $u = 0$ will bifurcate to an S^2 attractor*

Σ_λ for $\lambda > \lambda_0 = 1$. Furthermore, Σ_λ contains two stable equilibrium points and an unstable periodic orbit.

(iv) if $\ell \in \mathcal{I}_4$, then there exists k such that $\operatorname{Re} \beta_i(\lambda_0) = 0$, $i = k, k+1$ with $\rho^2 = 2/(k^2 + (k+1)^2)$ and $\lambda_0 = (1 - (k\rho)^2)^2$. Define parameters

$$(12) \quad \eta_1 = \frac{4b^2}{1 - \lambda_0} + \frac{2b^2(15(k\rho)^4 - 6(k\rho)^2)}{(15(k\rho)^4 - 6(k\rho)^2)^2 + (6\sigma(k\rho)^3)^2} - 3$$

$$(13) \quad \eta_2 = \frac{4b^2}{1 - \lambda_0} + \frac{4b^2((2k^2 - 2)\rho^2 - (k^4 - 1)\rho^4)}{((2k^2 - 2)\rho^2 - (k^4 - 1)\rho^4)^2 + (\sigma\rho^3(k^2 + 3k))^2} - 6$$

$$(14) \quad \eta_3 = \frac{4b^2}{1 - \lambda_0} + \frac{2b^2(15(k\rho + \rho)^4 - 6(k\rho + \rho)^2)}{(15(k\rho + \rho)^4 - 6(k\rho + \rho)^2)^2 + (6\sigma(k\rho + \rho)^3)^2} - 3.$$

If $k \geq 2$, then the transitions are as follows:

	$\eta_2 > 0$	$\eta_2 < 0$
$\eta_1 > 0, \eta_3 > 0$	catastrophic	continuous if $\eta_1\eta_3 < \eta_2^2$, catastrophic otherwise
$\eta_1 > 0, \eta_3 < 0$	catastrophic	mixed if $\eta_3 > \eta_2$ catastrophic otherwise
$\eta_1 < 0, \eta_3 < 0$	continuous if $\eta_1\eta_3 > \eta_2^2$, catastrophic otherwise	continuous

If $k = 1$, then the transition is continuous if $\eta_3 < 0$ and catastrophic if $\eta_3 > 0$. If the transition is continuous, then $u = 0$ bifurcates to an S^3 attractor for $\lambda > \lambda_0$.

Remark. Due to the double Hopf structure, in the case that the transition for $\ell \in \mathcal{I}_4$ is continuous, the bifurcated attractor Σ_λ contains two distinct periodic orbits as well as an invariant torus. The stability of these on the attractor depends on the transition parameters. See [5] for more details.

3. DYNAMIC TRANSITIONS

Now we are ready to give a full characterization of the dynamic transitions of Eq. (1).

3.1. Real Simple Transition. In the case that $\ell \in S_1$ or S_2 , we have real and complex simple eigenvalue transitions respectively. First consider the case that $m(\ell) = 1$.

Proposition 3.1. *If $\ell < 2\pi/\sqrt{2}$, then the transition at λ_0 is mixed if $b \neq 0$, and is continuous if $b = 0$.*

Proof. The center manifold is trivial. The trajectories on the center manifold simply consists of the solutions that depend only on time. At the transition $\lambda_0 = 1$, projecting onto the center manifold then gives the reduced system

$$\frac{du}{dt} = bu^2 - u^3$$

which implies that if $b > 0$, solutions with initial value $u(0) < 0$ will tend toward the fixed point at $u = 0$, and solutions with initial value $u(0) > 0$ will be repelled away. If $b < 0$ then we have the opposite behavior. Thus the transition is mixed for $b \neq 0$. If $b = 0$, $u = 0$ is then an asymptotically stable fixed point. Thus the transition will be continuous if $b = 0$. \square

3.2. Complex Simple Transition. Now consider the transition from complex simple eigenvalues. There will be a pair of conjugate eigenvalues that cross the imaginary axis as λ crosses λ_0 . Then there exists $\lambda_0 > 0$ and $k > 0$ so that $\beta_k = \bar{\beta}_{-k}$ and

$$\operatorname{Re}(\beta_i) = \begin{cases} < 0 & \text{if } \lambda < \lambda_0 \\ = 0 & \text{if } \lambda = \lambda_0 \\ > 0 & \text{if } \lambda > \lambda_0 \end{cases} \quad i = \pm k$$

$$\operatorname{Re}(\beta_i) < 0 \quad i \neq \pm k$$

Similar to before, we can split into subspaces

$$\begin{aligned} E_1 &= \operatorname{span}\{z\phi_k + \overline{z\phi_1} : z \in \mathbb{C}\} \\ E_2 &= E_1^\perp \text{ in } H^4(\mathbb{T}) \\ \bar{E}_2 &\text{ is the closure in } L^2(\mathbb{T}) \end{aligned},$$

and split the operator into $L_\lambda = \mathcal{J}_\lambda \oplus \mathcal{L}_\lambda$ so that $\mathcal{J}_\lambda = \operatorname{Diag}(\beta_k, \bar{\beta}_k)$.

Proposition 3.2. *The transition number for all $\ell \in S_2$ is given by*

$$(15) \quad P = \frac{2b^2}{(15^4 - 6(k\rho)^2) + 6\sigma(k\rho)^3i} + \frac{4b^2}{1 - \lambda_0} - 3.$$

Thus if b and σ are such that

$$(16) \quad \frac{2b^2(15(k\rho)^4 - 6(k\rho)^2)}{(15(k\rho)^4 - 6(k\rho)^2)^2 + (6\sigma(k\rho)^3)^2} + \frac{4b^2}{1 - \lambda_0} - 3 < 0$$

then the transition at $\lambda = \lambda_0$ will be continuous, for the reverse inequality, the transition will be catastrophic.

Proof. We begin by computing the center manifold. The center manifold is locally given by the graph of some map $\Phi(\cdot, \lambda) : E_1 \rightarrow \bar{E}_2$, which can be approximated by

$$(17) \quad \Phi(u, \lambda) = \int_{-\infty}^0 e^{-\tau \mathcal{L}_\lambda}(k\rho)_\epsilon P_2 G_2(e^{\tau \mathcal{J}_\lambda} u) d\tau + o(\|u\|^2)$$

where P_2 is the projection on to \bar{E}_2 , $u = z\phi_k + \overline{z\phi_k}$ for some $z \in \mathbb{C}$, and ρ_ϵ is a cutoff function so that we have compact support in E_1 . This formula is a generalization of the standard Lyapunov-Perron construction of invariant manifolds, see [8, 6, 5] for more details. First observe that

$$P_2 G(e^{\tau \mathcal{J}_\lambda} u) = be^{2\tau \beta_k} z^2 \phi_k^2 + be^{2\tau \bar{\beta}_k} \overline{z^2 \phi_k^2} + 2be^{\tau(\beta_k + \bar{\beta}_k)} z \phi_k \overline{z \phi_k}.$$

For λ near λ_0 , $\operatorname{Re}(2\beta_k - \beta_i) > 0$ and $\operatorname{Re}(\beta_k + \bar{\beta}_k - \beta_i) > 0$ for all $i \neq \pm k$. Therefore the integral in Eq. (17) converges. Then the center manifold function is given by

$$\begin{aligned} \Phi(u, \lambda) &= \frac{b}{2\beta_k - \beta_{2k}} z^2 \phi_k^2 + \frac{b}{2\beta_k - \beta_{2k}} \overline{z^2 \phi_k^2} + \frac{2b}{\beta_k + \bar{\beta}_k - \beta_0} z \phi_k \overline{z \phi_k} + o(\|u\|^2) \\ &= \frac{b}{[\lambda - (1 - (k\rho)^2)^2] - (6(k\rho)^2 - 15(k\rho)^4) + 6\sigma(k\rho)^3 i} z^2 \phi_k^2 \\ &\quad + \frac{b}{2[\lambda - (1 - (k\rho)^2)^2] + 1 - \lambda} |z|^2 + o(\|u\|^2) + c.c. \\ (18) \quad &=: Az^2 \phi_k^2 + B|z|^2 + o(\|u\|^2) + c.c. \end{aligned}$$

where $c.c.$ is the complex conjugate of everything before it. Let \mathcal{P}_k denote the projection onto ϕ_k , then

$$\mathcal{P}_k G(z\phi_k + \bar{z}\bar{\phi}_k + \Phi(u, \lambda)) = 2bAz|z|^2 + 4bBz|z|^2 - 3z|z|^2 + o(\|u\|^2)$$

Thus the dynamics on the center manifold projected onto ϕ_k at $\lambda = \lambda_0$ is given by the equation

$$\begin{aligned} \frac{dz}{dt} &= \mathcal{P}_k L_{\lambda_0}(z\phi_k + \bar{z}\bar{\phi}_k + \Phi(u, \lambda)) + \mathcal{P}_k G(z\phi_k + \bar{z}\bar{\phi}_k + \Phi(u, \lambda)) \\ &= \beta_k(\lambda_0)z + (2bA + 4bB - 3)z|z|^2 + o(\|u\|^3). \end{aligned}$$

This indeed satisfies all the assumptions of Theorem 2.2, and thus the transition number is given by $P = 2bA + 4bB - 3$. Note that

$$\lambda_0 - (1 - (k\rho)^2)^2 = 0$$

is it is when the eigenvalues cross the imaginary axis. Therefore we obtain the proposition upon substitution. \square

Part (iii) of Theorem 2.2 gives the bifurcated periodic solutions. So for continuous transitions, the system bifurcates to a stable periodic orbit for $\lambda > \lambda_0$, and for catastrophic transitions, the system bifurcates to an unstable periodic orbit for $\lambda < \lambda_0$.

3.3. Double Real-Complex Transition. Now we consider the single case of $\ell \in S_3$. Let $E_1 = \operatorname{span}\{z_0 + z_1\phi_1 + \overline{z_1\phi_1} : z_0 \in \mathbb{R}, z_1 \in \mathbb{C}\}$, and define E_2 as before. Split L_λ into \mathcal{J}_λ and \mathcal{L}_λ as before.

Proposition 3.3. *If $\ell \in S_3$, then the transition across $\lambda = \lambda_0$ is mixed for $b \neq 0$, and is continuous for $b = 0$.*

Proof. We express $u \in E_1$ as $u = z_0 + z_1\phi_1 + \overline{z_1\phi_1}$ where $z_0 \in \mathbb{R}$ and $z_1 \in \mathbb{C}$. Then

$$\begin{aligned} P_2 G_2(e^{\tau\mathcal{J}_\lambda} u) &= P_2 \left[b(e^{\tau\beta_0} z_0 + e^{\tau\beta_1} z_1\phi_1 + e^{\tau\bar{\beta}_1} \bar{z}_1\bar{\phi}_1)^2 \right] \\ &= be^{2\tau\beta_1} z_1^2 \phi_1^2 + be^{2\tau\bar{\beta}_1} \bar{z}_1^2 \bar{\phi}_1^2 \end{aligned}$$

Then the center manifold function is given by

$$\Phi(u, \lambda) = \frac{b}{2\beta_1 - \beta_2} z_1^2 \phi_1^2 + \frac{b}{2\bar{\beta}_1 - \bar{\beta}_2} \bar{z}_1^2 \bar{\phi}_1^2 + o((|z_0| + |z_1|)^2)$$

Note that if we project the dynamics onto ϕ_0 , we find

$$\frac{dz_0}{dt} = \beta_0 z_0 + \mathcal{P}_0(G(u + \Phi(u, \lambda))) = \beta_0 z_0 + b z_0^2 - z_0^3.$$

At $\lambda = \lambda_0 = 1$, this is the same situation as Section 3.1. Therefore for $b > 0$, trajectories with initial value whose ϕ_0 projection is positive will tend away from 0, and trajectories with initial value whose ϕ_0 projection is negative will tend toward 0. For $b < 0$, we again have the opposite behavior. Thus the transition is mixed if $b \neq 0$.

If $b = 0$, then $\Phi(u, \lambda) = o((|z_0| + |z_1|)^2)$. Then projecting onto ϕ_0 and ϕ_1 , we have the reduced system

$$(19) \quad \frac{dz_0}{dt} = \beta_0 z_0 - z_0^3$$

$$(20) \quad \frac{dz_1}{dt} = \beta_1 z_1 - z_0^2 z_1 - z_1 |z_1|^2 + o((|z_0| + |z_1|)^3).$$

Again we perform the change of variables to $z_1(t) = r(t)e^{i\gamma(t)}$ where $r(t) > 0$ and γ is a real function. Then substituting into Eq. (20) and taking the real part at $\lambda = \lambda_0 = 1$,

$$\frac{dr}{dt} = -z_0^2 r - r^3 + o((|z_0| + r)^3).$$

Since $r > 0$, this implies $\dot{r} < 0$. Eq. (19) implies that $\dot{z}_0 < 0$ as well, so $u = 0$ at $\lambda = \lambda_0$ is an asymptotically stable fixed point. Therefore the transition is continuous. \square

3.4. Double Complex Transition. Fix ℓ so that for some $k \geq 1$,

$$\text{Re}(\beta_i) = \begin{cases} < 0 & \text{if } \lambda < \lambda_0 \\ = 0 & \text{if } \lambda = \lambda_0 \\ > 0 & \text{if } \lambda > \lambda_0 \end{cases} \quad \begin{matrix} i = \pm k, \pm(k+1) \\ \\ i \neq \pm k, \pm(k+1) \end{matrix}$$

Define subspaces

$$E_1 = \text{span}\{z_1 \phi_k + \overline{z_1 \phi_1}, z_2 \phi_{k+1} + \overline{z_2 \phi_{k+1}} : z_1, z_2 \in \mathbb{C}\}$$

$$E_2 = E_1^\perp \text{ in } H^4(\mathbb{T})$$

$$\overline{E_2} \text{ is the closure in } L^2(\mathbb{T}).$$

Split $L_\lambda = \mathcal{J}_\lambda \oplus \mathcal{L}_\lambda$ so that $\mathcal{J}_\lambda = \text{Diag}(\beta_k, \overline{\beta_k}, \beta_{k+1}, \overline{\beta_{k+1}})$. Then for $u \in E_1$ (for which we can write as $z_1 \phi_k + \overline{z_1 \phi_1} + z_2 \phi_{k+1} + \overline{z_2 \phi_{k+1}}$ for some $z_1, z_2 \in \mathbb{C}$).

Proposition 3.4. *The system near $\lambda = \lambda_0$ is completely characterized by the projected system*

$$(21) \quad \frac{dz_1}{dt} = \beta_1(\lambda) z_1 + z_1(A(\lambda)|z_1|^2 + B(\lambda)|z_2|^2) + o((|z_1| + |z_2|)^3)$$

$$(22) \quad \frac{dz_2}{dt} = \beta_2(\lambda) z_2 + z_2(C(\lambda)|z_1|^2 + D(\lambda)|z_2|^2) + o((|z_1| + |z_2|)^3)$$

If $k > 1$, then the transition numbers are given by

$$\begin{aligned} A &= \frac{4b^2}{1 - \lambda_0} + \frac{2b^2}{(15(k\rho)^4 - 6(k\rho)^2) + 6\sigma(k\rho)^3 i} - 3 \\ B &= \frac{4b^2}{1 - \lambda_0} + \frac{4b^2}{(2k^2 - 2)\rho^2 - (k^4 - 1)\rho^4 + \sigma(3k^2 + 3k)\rho^3 i} - 6 \\ C &= \frac{4b^2}{1 - \lambda_0} + \frac{4b^2}{(2k^2 - 2)\rho^2 - (k^4 - 1)\rho^4 - \sigma(3k^2 + 3k)\rho^3 i} - 6 \\ D &= \frac{4b^2}{1 - \lambda_0} + \frac{2b^2}{(15(k\rho + \rho)^4 - 6(k\rho + \rho)^2) + 6\sigma(k\rho + \rho)^3 i} - 3 \end{aligned}$$

and if $k = 1$, the transition numbers are given by

$$\begin{aligned} A &= \frac{4b^2}{1 - \lambda_0} - 3 \\ B &= C = \frac{4b^2}{1 - \lambda_0} - 6 \\ D &= \frac{4b^2}{1 - \lambda_0} + \frac{2b^2}{(15(2\rho)^4 - 6(2\rho)^2) + 6\sigma(2\rho)^3 i} - 3 \end{aligned}$$

Proof. Again we first compute the center manifold function. Observe that for $u \in E_1$,

$$\begin{aligned} G_2(e^{\tau \mathcal{J}_\lambda u}) &= e^{2\tau\beta_k} z_1^2 \phi_k^2 + e^{2\tau\bar{\beta}_k} \bar{z}_1^2 \bar{\phi}_k^2 + e^{2\tau\beta_{k+1}} z_2^2 \phi_{k+1}^2 + e^{2\tau\bar{\beta}_{k+1}} \bar{z}_2^2 \bar{\phi}_{k+1}^2 \\ &\quad + 2 \left(e^{\tau(\beta_k + \bar{\beta}_k)} z_1 \bar{z}_1 \phi_k \bar{\phi}_k + e^{\tau\beta_{k+1} + \bar{\beta}_{k+1}} z_2 \bar{z}_2 \phi_{k+1} \bar{\phi}_{k+1} \right. \\ &\quad \left. + e^{\tau(\beta_k + \bar{\beta}_{k+1})} z_1 \bar{z}_2 \phi_k \bar{\phi}_{k+1} + e^{\tau(\bar{\beta}_k + \beta_{k+1})} \bar{z}_1 z_2 \bar{\phi}_k \phi_{k+1} \right) \end{aligned}$$

It is clear from above that $P_2 G_2(e^{\tau \mathcal{J}_\lambda u}) = G_2(e^{\tau \mathcal{J}_\lambda u})$ for $k \neq 1$, and for $k = 1$, several cross terms will vanish. We consider the case $k \neq 1$ first. Projecting onto E_2 and integrating τ from $-\infty$ to 0, we find

$$\begin{aligned} (23) \quad \Phi(u, \lambda) &= \frac{b}{2\beta_k - \beta_{2k}} z_1^2 \phi_k^2 + \frac{b}{2\beta_{k+1} - \beta_{2k+2}} z_2^2 \phi_{k+1}^2 + \frac{b}{\beta_k + \bar{\beta}_k - \beta_0} |z_1|^2 \\ &\quad + \frac{b}{\beta_{k+1} + \bar{\beta}_{k+1} - \beta_0} |z_2|^2 + \frac{2b}{\bar{\beta}_k + \beta_{k+1} - \beta_1} \bar{z}_1 z_2 \phi_1 + o((|z_1| + |z_2|)^2) + c.c. \end{aligned}$$

where $c.c.$ is the complex conjugate of everything preceding it. Label the coefficients in Eq. (23) μ_i for i from 1 to 5 so that

$$\Phi(u, \lambda) = \mu_1 z_1^2 \phi_k^2 + \mu_2 z_2^2 \phi_{k+1}^2 + \mu_3 |z_1|^2 + \mu_4 |z_2|^2 + \mu_5 \bar{z}_1 z_2 \phi_1 + c.c.$$

Note that μ_3 and μ_4 are real, and all of them depend on λ and the fixed parameters b and σ . Note that at $\lambda_0 - (1 - (k\rho)^2)^2 = 0$ and $\lambda_0 - (1 - (k\rho + \rho)^2)^2 = 0$. So at

$\lambda = \lambda_0$, the coefficients are given by

$$\begin{aligned}\mu_1 &= \frac{b}{15(k\rho)^4 - 6(k\rho)^2 + 6\sigma(k\rho)^3 i} \\ \mu_4 &= \frac{b}{15(k\rho + \rho)^4 - 6(k\rho + \rho)^2 + 6\sigma(k\rho + \rho)^3 i} \\ \mu_2 &= \mu_3 = \frac{b}{1 - \lambda_0} \\ \mu_5 &= \frac{2b}{(2k^2 - 2)\rho^2 - (k^4 - 1)\rho^4 - \sigma(3k^2 + 3k)\rho^3 i}\end{aligned}$$

The complex system yielded from projecting the dynamics on the center manifold onto ϕ_k and ϕ_{k+1} completely captures the dynamics of the real system. Let \mathcal{P}_k and \mathcal{P}_{k+1} denote the projections onto ϕ_k and ϕ_{k+1} respectively. Then

$$\begin{aligned}\mathcal{P}_k G(z_1 \phi_k + z_2 \phi_{k+1} + \overline{z_1 \phi_k} + \overline{z_2 \phi_{k+1}} + \Phi(u, \lambda)) &= (4b\mu_3 + 2b\mu_1 - 3)z_1|z_1|^2 \\ &\quad + (4b\mu_4 + 2b\overline{\mu}_5 - 6)z_1|z_2|^2 + o((|z_1| + |z_2|)^3)\end{aligned}$$

and

$$\begin{aligned}\mathcal{P}_{k+1} G(z_1 \phi_k + z_2 \phi_{k+1} + \overline{z_1 \phi_k} + \overline{z_2 \phi_{k+1}} + \Phi(u, \lambda)) &= (4b\mu_3 + 2b\mu_5 - 6)z_2|z_1|^2 \\ &\quad + (4b\mu_4 + 2b\mu_2 - 3)z_2|z_2|^2 + o((|z_1| + |z_2|)^3)\end{aligned}$$

Now for $k = 1$,

$$P_2 G_2(e^{\tau \mathcal{I}_\lambda} u) = e^{2\tau\beta_2} z_2 \phi_2^2 + e^{\tau(\beta_1 + \overline{\beta}_1)} |z_1| + e^{\tau(\beta_2 + \overline{\beta}_2)} |z_2| + c.c.$$

So then

$$\Phi(u, \lambda) = \frac{b}{2\beta_2 - \beta_4} z_2^2 \phi_2^2 + \frac{b}{\beta_1 + \overline{\beta}_1 - \beta_0} |z_1|^2 + \frac{b}{\beta_2 + \overline{\beta}_2 - \beta_0} |z_2|^2 + o((|z_1| + |z_2|)^2) + c.c.$$

Label the coefficients ν_i so that $\Phi(u, \lambda) = \nu_1 z_2^2 \phi_2^2 + \nu_2 |z_1|^2 + \nu_3 |z_2|^2 + o((|z_1| + |z_2|)^2) + c.c.$. Then

$$\begin{aligned}\mathcal{P}_1 G(z_1 \phi_1 + z_2 \phi_2 + \overline{z_1 \phi_1} + \overline{z_2 \phi_2} + \Phi(u, \lambda)) &= (4b\nu_2 - 3)z_1|z_1|^2 \\ &\quad + (4b\nu_3 - 6)z_1|z_2|^2 + o((|z_1| + |z_2|)^3)\end{aligned}$$

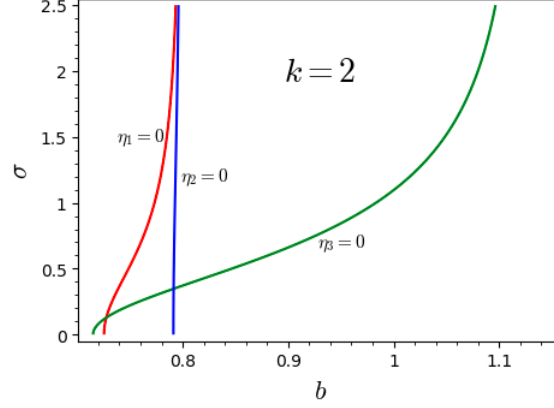
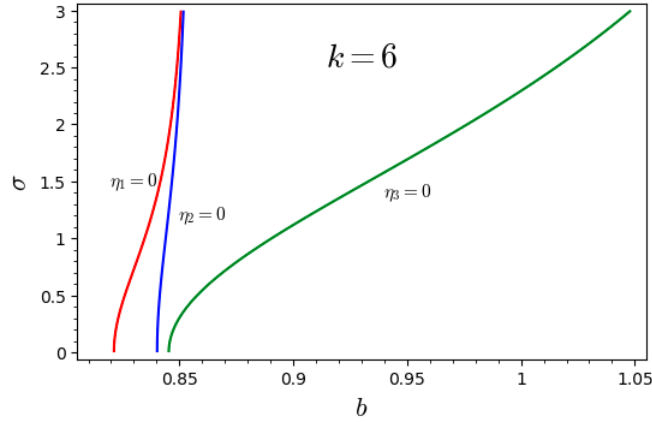
$$\begin{aligned}\mathcal{P}_2 G(z_1 \phi_1 + z_2 \phi_2 + \overline{z_1 \phi_1} + \overline{z_2 \phi_2} + \Phi(u, \lambda)) &= (4b\nu_2 - 6)z_2|z_1|^2 \\ &\quad + (4b\nu_3 + 2b\nu_1 - 3)z_2|z_2|^2 + o((|z_1| + |z_2|)^3)\end{aligned}$$

Substituting in the values for μ_i and ν_j at $\lambda = \lambda_0$, we have the desired result. \square

Note that $\text{Re } B = \text{Re } C$. The parameters given in Eq. (12) - (14) are given by

$$\eta_1 = \text{Re } A, \quad \eta_2 = \text{Re } B = \text{Re } C, \quad \eta_3 = \text{Re } D.$$

Note that for a fixed value of σ , $\eta_1(b) > \eta_3(b)$. Then applying Theorem 2.3 immediately yields part (iv) of Theorem 2.4.

FIGURE 4. Phase diagram for $k = 2$.FIGURE 5. Phase diagram for $k = 6$.

4. REAL CENTER MANIFOLD FUNCTION AND NUMERICAL RESULTS

So far, to classify the types of transition, it has benefitted us to work in a complex space since rotational behavior is much more simply described in complex spaces, thus giving us simple forms for the transition number (compared to the standard bifurcation number formula [5] for Hopf bifurcation). However, the physics of the system still resides in a real space. A particularly simple case with nontrivial transitions to analyze is the case $\ell = 2\pi$. In this section, we give the explicit formula for the center manifold function in a real function space for this case, and numerically compute the approximate trajectories on the center manifold.

Define E_1 and E_2 as in Section 3.2.

Proposition 4.1. *The center manifold function $\Phi : E_1 \rightarrow \overline{E}_2$ of Eq. (1) with $\ell = 2\pi$ is locally approximated by*

$$(24) \quad \Phi(u, \lambda)(x) = A(u) \cos(2x) + B(u) \sin(2x) + C(u) + o(\|u\|^2)$$

where $u = u_1 \cos(x) + u_2 \sin(x)$ and

$$\begin{aligned} A(u) &= A(u_1, u_2) := \frac{1}{2} \frac{b}{(\lambda + 9)^2 + (6\sigma)^2} ((9 + \lambda)(u_1^2 - u_2^2) - 12u_1 u_2 \sigma) \\ B(u) &= B(u_1, u_2) := \frac{1}{2} \frac{b}{(\lambda + 9)^2 + (6\sigma)^2} ((9 + \lambda)2u_1 u_2 + 6\sigma(u_1^2 - u_2^2)) \\ C(u) &= C(u_1, u_2) := \frac{b}{2(\lambda + 1)}(u_1^2 + u_2^2) \end{aligned}$$

for λ near 0.

Note that A , B , and C are all $O(\|u\|^2)$.

Proof. Assume $\ell = 2\pi$. Then we have

$$\beta_n(\lambda) = \lambda - (1 - n^2)^2 - i\sigma n^3.$$

From Eq. (18)

$$\begin{aligned} \Phi(u, \lambda) &= \frac{b}{2\beta_1 - \beta_2} z^2 \phi_1^2 + \frac{b}{2\beta_1 - \beta_2} \overline{z^2 \phi_1^2} + \frac{2b}{\beta_1 + \overline{\beta_1} - \beta_0} z \phi_1 \overline{z \phi_1} + o(\|u\|^2) \\ (25) \quad &= 2\operatorname{Re} \left(\frac{b}{\lambda + 9 + 6\sigma i} z^2 \phi_1^2 \right) + \frac{2b}{\lambda + 1} |z|^2 + o(\|u\|^2) \end{aligned}$$

We wish to express the center manifold function in the o.n.b. for E_1 given by

$$e_1 = \cos x \quad e_2 = \sin x,$$

so $u = u_1 e_1 + u_2 e_2$ for some $u_1, u_2 \in \mathbb{R}$, and it is clear that

$$z = \frac{1}{2}(u_1 - iu_2).$$

We want to express the center manifold function as a function of u_1 and u_2 . First note that the second term of Eq. (25) rearranges pretty easily to

$$(26) \quad \frac{b}{\lambda + 1} |z|^2 = \frac{b}{4(\lambda + 1)} (u_1^2 + u_2^2).$$

For the first term of Eq. (25), we have

$$\begin{aligned} \operatorname{Re} \left[\frac{bz^2}{\lambda + 9 + 6\sigma i} \phi_1^2 \right] &= \operatorname{Re} \left[\frac{bz^2}{\lambda + 9 + 6\sigma i} (e_1 + ie_2)^2 \right] \\ &= \frac{1}{4} \frac{b}{(\lambda + 9)^2 + (6\sigma)^2} \operatorname{Re} [(\lambda + 9 - 6\sigma i)(u_1 - iu_2)^2 (e_1 + ie_2)^2] \\ &= \frac{1}{4} \frac{b}{(\lambda + 9)^2 + (6\sigma)^2} [((9 + \lambda)(u_1^2 - u_2^2) - 12u_1 u_2 \sigma) \cos(2x) \\ (27) \quad &+ ((9 + \lambda)2u_1 u_2 + 6\sigma(u_1^2 - u_2^2)) \sin(2x)] \end{aligned}$$

The center manifold function is then simply twice the sum of the real parts of either term, so putting Eq. (26) and Eq. (27) together,

$$\begin{aligned}\Phi(u_1, u_2, \lambda)(x) &= \frac{b}{2(\lambda + 1)}(u_1^2 + u_2^2) \\ &+ \frac{1}{2} \frac{b}{(\lambda + 9)^2 + (6\sigma)^2} [((9 + \lambda)(u_1^2 - u_2^2) - 12u_1u_2\sigma) \cos(2x) \\ &+ ((9 + \lambda)2u_1u_2 + 6\sigma(u_1^2 - u_2^2)) \sin(2x)] + o(\|u\|^2),\end{aligned}$$

which completes the proof. \square

From the center manifold function, we now compute the reduced system. Let \mathcal{P}_1 and \mathcal{P}_2 denote the projection onto e_1 and e_2 respectively.

Proposition 4.2. *The dynamics on the center manifold can be locally approximated by is then given by*

$$\begin{aligned}\frac{du_1}{dt} &= \lambda u_1 - \sigma u_2 + 2bu_1C(u_1, u_2) + bu_1A(u_1, u_2) \\ &+ bu_2B(u_1, u_2) - \frac{3}{4}u_1^3 - \frac{3}{4}u_1u_2^2\end{aligned}\tag{28}$$

$$\begin{aligned}\frac{du_2}{dt} &= \sigma u_1 + \lambda u_2 + bu_1B(u_1, u_2) - bu_2A(u_1, u_2) \\ &+ 2bu_2C(u_1, u_2) - \frac{3}{4}u_2^3 - \frac{3}{4}u_1^2u_2\end{aligned}\tag{29}$$

where u_1 and u_2 are the amplitudes of projection onto e_1 and e_2 respectively.

Proof. Projecting the dynamics on the center manifold onto the center subspace, we find the reduced system

$$(30) \quad \begin{cases} \frac{du_1}{dt} = \mathcal{P}_1 \mathcal{L}_\lambda(u_1e_1 + u_2e_2) + \mathcal{P}_1 G(u_1e_1 + u_2e_2 + \Phi(u_1e_1 + u_2e_2, \lambda)) \\ \frac{du_2}{dt} = \mathcal{P}_2 \mathcal{L}_\lambda(u_1e_1 + u_2e_2) + \mathcal{P}_2 G(u_1e_1 + u_2e_2 + \Phi(u_1e_1 + u_2e_2, \lambda)) \end{cases}.$$

Observe that

$$\begin{aligned}\mathcal{L}_\lambda(u_1e_1 + u_2e_2) &= \mathcal{L}_\lambda(z\phi_1 + \overline{z\phi_1}) \\ &= (\lambda - i\sigma)z\phi_1 + \overline{(\lambda - i\sigma)z\phi_1} \\ &= (\lambda u_1 - \sigma u_2)e_1 + (\sigma u_1 + \lambda u_2)e_2\end{aligned}\tag{31}$$

For the projection of G onto $e_1(x)$, we find that

$$\begin{aligned}
\mathcal{P}_1 G(u_1 e_1 + u_2 e_2 + \Phi) &= \mathcal{P}_1 (2bu_1 u_2 e_1 e_2 + 2bu_1 e_1 \Phi + 2bu_2 e_2 \Phi \\
&\quad + bu_1^2 e_1^2 + bu_2^2 e_2^2 - u_1^3 e_1^3 - u_2^3 e_2^3 \\
&\quad - 3u_1^2 u_2 e_1^2 e_2 - 3u_1 u_2^2 e_1 e_2^2) + o(\|u\|^3) \\
&= \frac{1}{\pi} \int_0^{2\pi} (2bu_1 e_1 \Phi + 2bu_2 e_2 \Phi - u_1^3 e_1^3 - 3u_1 u_2^2 e_1 e_2^2) e_1 dx \\
&\quad + o(\|u\|^3) \\
&= 2bu_1 C(u_1, u_2) + bu_1 A(u_1, u_2) + bu_2 B(u_1, u_2) \\
&\quad - \frac{3}{4} u_1^3 - \frac{3}{4} u_1 u_2^2 + o(\|u\|^3).
\end{aligned} \tag{32}$$

For the projection onto $e_2(x)$, we similarly find

$$\begin{aligned}
\mathcal{P}_2 G(u_1 e_1 + u_2 e_2 + \Phi) &= \mathcal{P}_2 (2bu_1 u_2 e_1 e_2 + 2bu_1 e_1 \Phi + 2bu_2 e_2 \Phi \\
&\quad + bu_1^2 e_1^2 + bu_2^2 e_2^2 - u_1^3 e_1^3 - u_2^3 e_2^3 \\
&\quad - 3u_1^2 u_2 e_1^2 e_2 - 3u_1 u_2^2 e_1 e_2^2) + o(\|u\|^3) \\
&= \frac{1}{\pi} \int_0^{2\pi} (2bu_1 e_1 \Phi + 2bu_2 e_2 \Phi - u_2^3 e_2^3 - 3u_1^2 u_2 e_1^2 e_2) e_2 dx \\
&\quad + o(\|u\|^3) \\
&= bu_1 B(u_1, u_2) - bu_2 A(u_1, u_2) + 2bu_2 C(u_1, u_2) \\
&\quad - \frac{3}{4} u_2^3 - \frac{3}{4} u_1^2 u_2 + o(\|u\|^3).
\end{aligned} \tag{33}$$

So then putting Eq. (31)-(33) into Eq. (30), we find an approximate reduced system that locally describes the dynamics:

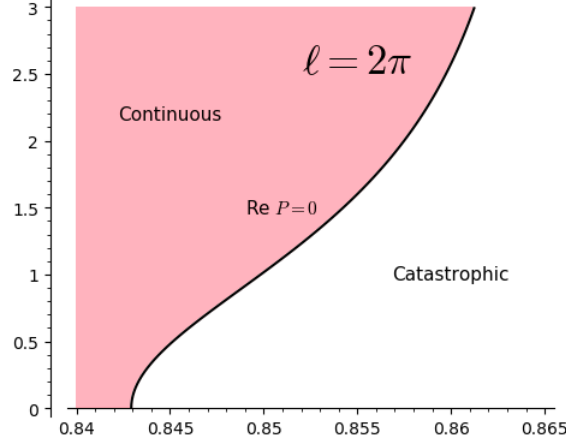
$$\begin{aligned}
\frac{du_1}{dt} &= \lambda u_1 - \sigma u_2 + 2bu_1 C(u_1, u_2) + bu_1 A(u_1, u_2) \\
&\quad + bu_2 B(u_1, u_2) - \frac{3}{4} u_1^3 - \frac{3}{4} u_1 u_2^2
\end{aligned} \tag{34}$$

$$\begin{aligned}
\frac{du_2}{dt} &= \sigma u_1 + \lambda u_2 + bu_1 B(u_1, u_2) - bu_2 A(u_1, u_2) \\
&\quad + 2bu_2 C(u_1, u_2) - \frac{3}{4} u_2^3 - \frac{3}{4} u_1^2 u_2
\end{aligned} \tag{35}$$

□

For completeness and to verify that this is indeed the same as what we computed in Section 3.2, we directly compute the Lyapunov number associated with the Hopf bifurcation that occurs at λ_0 . Note that Eq. (32) and Eq. (33) can be rearranged to a polynomial u_1 and u_2 so that

$$\mathcal{P}_i G(u_1 e_1 + u_2 e_2 + \Phi(u_1 e_1 + u_2 e_2, \lambda_0)) = \sum_{2 \leq p+q \leq 3} a_{pq}^i u_1^p u_2^q + o(\|u\|^3)$$

FIGURE 6. The phase diagram at $\ell = 2\pi$.

for $i = 1, 2$. Then the Lyapunov number is given by

$$\begin{aligned} \eta = & \frac{3\pi}{4}(a_{30}^1 + a_{03}^2) + \frac{\pi}{4}(a_{12}^1 + a_{21}^2) + \frac{\pi}{2\text{Im}(\bar{\beta}_1)}(a_{02}^1 a_{02}^2 - a_{20}^1 a_{20}^2) \\ & + \frac{\pi}{4\text{Im}(\bar{\beta}_1)}(a_{11}^1 a_{20}^1 + a_{11}^1 a_{02}^1 - a_{11}^2 a_{20}^2 - a_{11}^2 a_{02}^2). \end{aligned}$$

It is easy to see by inspection that $a_{pq}^i = 0$ for all $p + q = 2$, and

$$\begin{aligned} a_{30}^1 &= a_{03}^2 = -\frac{3}{4} + b^2 + \frac{1}{2} \frac{b^2}{9 + 4\sigma^2} \\ a_{12}^1 &= a_{21}^2 = -\frac{3}{4} + b^2 + \frac{1}{2} \frac{b^2}{9 + 4\sigma^2} \end{aligned}$$

Then following the bifurcation number formula, we find

$$\eta = \pi \left(2b^2 + \frac{b^2}{9 + 4\sigma^2} - \frac{3}{2} \right)$$

Therefore we have a continuous transition if $\eta < 0$, so we have a continuous transition if

$$4b^2 + \frac{2b^2}{9 + 4\sigma^2} - 3 < 0$$

and a catastrophic transition for the opposite inequality (see Fig. 6). This implies that if $b^2 < \frac{27}{38}$, the transition will be continuous, if $b^2 > \frac{3}{4}$, the transition will necessarily be a catastrophic transition. Note that this indeed matches the results of Section 3.2.

We can see the change in the transition type across a critical value of σ . Take $b = 0.86$, then the critical value is at $\sigma \approx 2.577$. So at $\sigma = 2.6$, we expect to see a continuous transition, with attracting periodic orbits for $\lambda > 0$. And indeed, at $\lambda = 0.01$, we see in the left side graph of Fig. 7 that the forward in time solutions

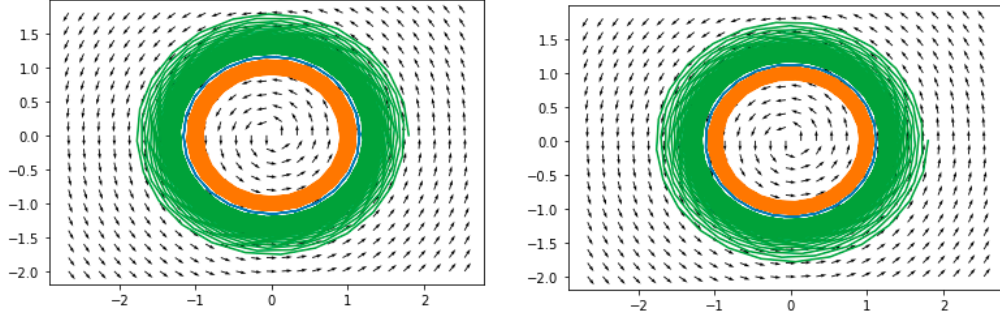


FIGURE 7. Forward in time trajectories (left) tending towards the stable periodic orbit (blue), and backward in time trajectories (right) tending towards the unstable periodic orbit (blue).

(up to $t = 100$) with initial values at $(0.9, 0)$ and $(1.8, 0)$ converge onto a limit cycle, approximated by $r \approx 1.158$.

At $\sigma = 2.5$, we expect a catastrophic transition, with repelling periodic orbits for $\lambda < 0$. At $\lambda = -0.1$, we see in the right side graph of Fig. 7 that the backward in time solutions with initial values at $(0.9, 0)$ and $(0.8, 0)$ also converge onto a limit cycle, approximated by $r \approx 1.122$.

For continuous transitions, we can also numerically approximate the radius of the limit cycles for small values of lambda by simply performing a binary search. As $\lambda \rightarrow 0$, the radius should decrease as the square root of lambda with coefficient determined by $\text{Re } P$ as in Theorem 2.2. And indeed, we can see this behavior clearly at $\sigma = 6$ and $b = 0.86$ in Fig. 8.

The special case of $\ell = 2\pi$ came with a lot of computational conveniences. However, it is easy to see that the dynamics for other $\ell \in \mathcal{I}_2$ follow similar dynamics, and the line $\text{Re } P = 0$ in $\sigma - b$ phase space takes the same shape. Lastly, we give the real center manifold formulas for $\ell \in \mathcal{I}_2$ and \mathcal{I}_4 in real coordinates. Recall from Eq. (18) that the center manifold function for $\ell \in \mathcal{I}_2$ is given by

$$\begin{aligned} \Phi(u, \lambda) &= \frac{b}{2\beta_k - \beta_{2k}} z^2 \phi_k^2 + \frac{b}{2\beta_k - \beta_{2k}} \overline{z^2 \phi_k^2} + \frac{2b}{\beta_k + \overline{\beta_k} - \beta_0} z \phi_k \overline{z \phi_k} + o(\|u\|^2) \\ &= 2 \text{Re} \left(\frac{b}{[\lambda - (1 - \rho^2)^2] - (6\rho^2 - 15\rho^4) + 6\sigma\rho^3 i} z^2 \phi_k^2 \right) \\ &\quad + \frac{2b}{2[\lambda - (1 - \rho^2)^2] + 1 - \lambda} |z|^2 + o(\|u\|^2). \end{aligned}$$

Then employing the same change of basis with

$$e_1 = \cos(kx), \quad e_2 = \sin(kx)$$

so that $u = u_1 e_1 + u_2 e_2$ and $z = \frac{1}{2}(u_1 - i u_2)$, we find the following formula:

Proposition 4.3. *The center manifold function for $\ell \in \mathcal{I}_2$ for Eq. (1) is given by*

$$\Phi(u_1, u_2, \lambda)(x) = A(u_1, u_2, \lambda) \cos(2kx) + B(u_1, u_2, \lambda) \sin(2kx) + C(u_1, u_2, \lambda)$$

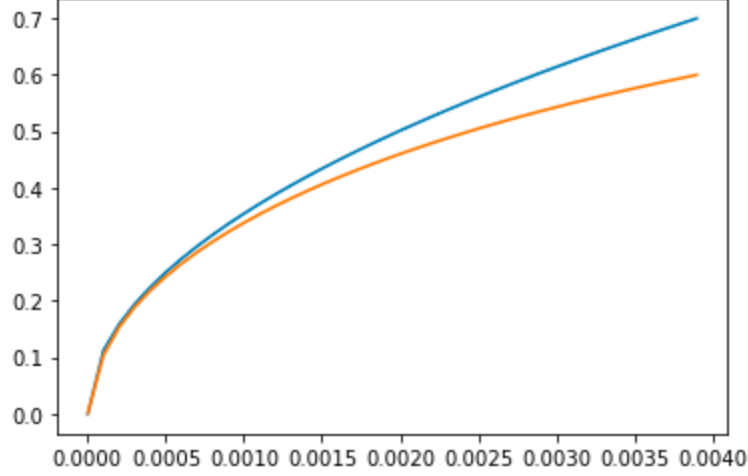


FIGURE 8. The blue line is the numerical approximations of the radius of the limit cycles as a function of λ , and the orange line is the analytical limiting behavior as $\lambda \rightarrow 0$.

where

$$A(u_1, u_2, \lambda) = \frac{1}{2} \frac{b}{([\lambda - (1 - \rho^2)]^2 - (15\rho^4 - 6\rho^2))^2 + (6\sigma\rho^3)^2} \cdot [([\lambda - (1 - \rho^2)]^2 - (15\rho^4 - 6\rho^2)) (u_1^2 - u_2^2) - 12u_1u_2\sigma\rho^3]$$

$$B(u_1, u_2, \lambda) = \frac{1}{2} \frac{b}{([\lambda - (1 - \rho^2)]^2 - (15\rho^4 - 6\rho^2))^2 + (6\sigma\rho^3)^2} \cdot [([\lambda - (1 - \rho^2)]^2 - (15\rho^4 - 6\rho^2)) 2u_1u_2 + 6\sigma\rho^3(u_1^2 - u_2^2)]$$

$$C(u_1, u_2, \lambda) = \frac{1}{2} \frac{b}{2[\lambda - (1 - \rho^2)]^2 + 1 - \lambda} (u_1^2 + u_2^2)$$

Now for $\ell \in \mathcal{I}_4$. Then the center manifold function in the complex eigenbasis was given by Eq. (23). We want to change basis to

$$e_1 = \cos(kx) \quad e_2 = \sin(kx) \quad e_3 = \cos((k+1)x) \quad e_4 = \sin((k+1)x).$$

We can write $u = \sum_{i=1}^4 u_i e_i$, so that

$$z_1 = \frac{1}{2}(u_1 - iu_2) \quad z_2 = \frac{1}{2}(u_3 - iu_4)$$

Let

$$\begin{aligned} c_1 + d_1 i &:= \frac{b}{2\beta_k - \beta_{2k}} \\ c_2 + d_2 i &:= \frac{b}{2\beta_{k+1} - \beta_{2k+2}} \\ c_3 &:= \frac{b}{\beta_k + \bar{\beta}_k - \beta_0} \\ c_4 &:= \frac{b}{\beta_{k+1} + \bar{\beta}_{k+1} - \beta_0} \\ c_5 + d_5 i &:= \frac{2b}{\bar{\beta}_k + \beta_{k+1} - \beta_1}. \end{aligned}$$

Note that c_i and d_i depend on λ for some fixed ℓ and σ . Substituting into the center manifold function,

$$\begin{aligned} \Phi(u_1, u_2, u_3, u_4, \lambda) = 2 \operatorname{Re} & \left[\frac{1}{4}(c_1 + id_1)(u_1 - iu_2)^2(\cos(2kx) + i\sin(2kx)) \right. \\ & + \frac{1}{4}(c_2 + id_2)(u_3 - iu_4)^2(\cos((2k+2)x) + i\sin((2k+2)x)) \\ & + \frac{1}{4}c_3(u_1^2 + u_2^2) + \frac{1}{4}c_4(u_3^2 + u_4^2) \\ & \left. + \frac{1}{4}(c_5 + id_5)(u_1 + iu_2)(u_3 - iu_4)(\cos x + i\sin x) \right] \end{aligned}$$

This can be rearranged to yield the following:

Proposition 4.4. *The center manifold function for $\ell \in \mathcal{I}_4$ is given by*

$$\begin{aligned} \Phi(u, \lambda) = A_1 \cos(2kx) + A_2 \sin(2kx) + B_1 \cos((2k+2)x) \\ + B_2 \sin((2k+2)x) + C + D_1 \cos x + D_2 \sin(x) \end{aligned}$$

where

$$\begin{aligned} A_1 &= c_1(u_1^2 - u_2^2) + 2d_1 u_1 u_2 & A_2 &= 2c_1 u_1 u_2 - d_1(u_1^2 - u_2^2) \\ B_1 &= c_2(u_3^2 - u_4^2) + 2d_2 u_3 u_4 & B_2 &= 2c_2 u_3 u_4 - d_2(u_3^2 - u_4^2) \\ C &= \frac{1}{4}c_3(u_1^2 + u_2^2) + \frac{1}{4}c_4(u_3^2 + u_4^2) \\ D_1 &= c_5(u_1 u_3 + u_2 u_4) + d_5(u_1 u_4 - u_2 u_3) \\ D_2 &= c_5(u_1 u_4 - u_2 u_3) - d_5(u_1 u_3 + u_2 u_4) \end{aligned}$$

Thus Proposition 4.3 and Proposition 4.3 gives the real manifolds on which the exchange of stability occurs for all $\ell > 2\pi/\sqrt{2}$.

ACKNOWLEDGEMENTS

This research was funded by NSF / DMS grant 1757857 as part of the 2020 Indiana Research Experiences for Undergraduates (REU) Program. The author greatly

thanks Shouhong Wang for not only suggesting the problem, but also providing resources and support over the weeks spent on the problem. He would also like to thank Dylan Thurston for running the REU program despite all the challenges presented by Covid-19 outbreak.

REFERENCES

- [1] Jongmin Han and Chun-Hsiung Hsia. Dynamical bifurcation of the two dimensional swift-hohenberg equation with odd periodic condition. *Discrete and Continuous Dynamical Systems. Series B*, 7, 10 2012.
- [2] A. Hariz, L. Bahloul, L. Cherbi, K. Panajotov, M. Clerc, M. A. Ferré, B. Kostet, E. Averlant, and M. Tlidi. Swift-hohenberg equation with third-order dispersion for optical fiber resonators. *Phys. Rev. A*, 100:023816, Aug 2019.
- [3] Tung Hoang and Hyung Hwang. Dynamic pattern formation in swift-hohenberg equations. *Quarterly of Applied Mathematics*, 69, 07 2011.
- [4] Chanh Kieu, Taylan Sengul, Quan Wang, and Dongming Yan. On the hopf (double hopf) bifurcations and transitions of two-layer western boundary currents. *Communications in Nonlinear Science and Numerical Simulation*, 65, 05 2018.
- [5] T. Ma and S. Wang. *Bifurcation Theory and Applications*. Bifurcation Theory and Applications. World Scientific, 2005.
- [6] Tian Ma and Shouhong Wang. Bifurcation and stability of superconductivity. *Journal of Mathematical Physics*, 46(9):095112, 2005.
- [7] Tian Ma and Shouhong Wang. *Phase transition dynamics*. 11 2013.
- [8] Taylan Sengul and Shouhong Wang. Dynamic transitions and baroclinic instability for 3d continuously stratified boussinesq flows. *Journal of Mathematical Fluid Mechanics*, 20(3):1173–1193, September 2018.

DEPARTMENT OF MATHEMATICS, YALE UNIVERSITY, NEW HAVEN, CT 06510, USA
E-mail address, Kevin Li: `k.li@yale.edu`